M. MOSIAŁEK*, M. TATKO*, M. DUDEK**, E. BIELAŃSKA*, G. MORDARSKI*

COMPOSITE Ag-La$_{0.6}$Sr$_{0.4}$Co$_{0.8}$Fe$_{0.2}$O$_{3-\delta}$ CATHODE MATERIAL FOR SOLID OXIDE FUEL CELLS, PREPARATION AND CHARACTERISTIC

KOMPOZYTOWY MATERIAŁ KATODOWY Ag-La$_{0.6}$Sr$_{0.4}$Co$_{0.8}$Fe$_{0.2}$O$_{3-\delta}$ DO STAŁOTLENKOWYCH OGNIW PALIWOWYCH, OTRZYMYWANIE I CHARAKTERYSTYKA

Composite cathodes Ag-La$_{0.6}$Sr$_{0.4}$Co$_{0.2}$Fe$_{0.8}$O$_{3-\delta}$ were obtained by two different procedures. In the first procedure porous La$_{0.6}$Sr$_{0.4}$Co$_{0.2}$Fe$_{0.8}$O$_{3-\delta}$ (LSCF) matrix was prepared by sintering the LSCF paste, the matrix was then saturated with AgNO$_3$ solution and sintered again. Introduced silver crystalized in the form of 10 nm crystallites in the whole LSCF matrix. In the second procedure the paste of silver powder was deposited on the surface of electrolyte and dried. The layer of silver paste was then covered by a layer of the LSCF paste and sintered at 850°C. The following cells were tested: H$_2$|Ni-Ce$_{0.8}$Gd$_{0.2}$O$_{1.9}$|Ce$_{0.8}$Sm$_{0.2}$O$_{1.9}$ |LSCF|O$_2$, H$_2$|Ni-Ce$_{0.8}$Gd$_{0.2}$O$_{1.9}$|Ce$_{0.8}$Sm$_{0.2}$O$_{1.9}$|LSCF-Ag|O$_2$ and H$_2$|Ni-Ce$_{0.8}$Gd$_{0.2}$O$_{1.9}$|Ce$_{0.8}$Sm$_{0.2}$O$_{1.9}$|Ag|LSCF|O$_2$. Introduction of silver interlayer between cathode and electrolyte increased output power by 18-28% whereas introduction of metallic silver into porous LSCF caused increase in power by 14-18%.

Keywords: intermediate temperature solid oxide fuel cell, Ag-LSCF composite cathode, silver interlayer, samaria doped ceria

Kompozytowe katody Ag-La$_{0.6}$Sr$_{0.4}$Co$_{0.2}$Fe$_{0.8}$O$_{3-\delta}$ wykonano dwoma sposobami. W pierwszej metodzie otrzymano porowatą matrycę La$_{0.6}$Sr$_{0.4}$Co$_{0.2}$Fe$_{0.8}$O$_{3-\delta}$ (LSCF) poprzez wyprażenie pasty LSCF, następnie nasączono ją roztworem AgNO$_3$ i ponownie wyprażono. Wprowadzone srebro wykrystalizowało w postaci 10 nm krystalitów w matrycy LSCF. W drugiej metodzie na powierzchni elektrolitu położono pastę srebrną a po wysuszeniu pastę LSCF i wyprażono w 850°C. Testowano następujące ogniwa H$_2$|Ni-Ce$_{0.8}$Gd$_{0.2}$O$_{1.9}$ |Ce$_{0.8}$Sm$_{0.2}$O$_{1.9}$|LSCF|O$_2$, H$_2$|Ni-Ce$_{0.8}$Gd$_{0.2}$O$_{1.9}$|Ce$_{0.8}$Sm$_{0.2}$O$_{1.9}$|LSCF-Ag|O$_2$ i H$_2$|Ni-Ce$_{0.8}$Gd$_{0.2}$O$_{1.9}$|Ce$_{0.8}$Sm$_{0.2}$O$_{1.9}$|Ag|LSCF|O$_2$. Wprowadzenie warstwy srebra pomiędzy katodę a elektrolit podniosło moc ogniwa o 18-28% podczas gdy wprowadzenie srebra do porowatego LSCF spowodowało wzrost mocy o 14-18%.

1. Introduction

La$_{0.6}$Sr$_{0.4}$Co$_{0.2}$Fe$_{0.8}$O$_{3-\delta}$ (LSCF) shows very high catalytic activity in the oxygen reduction reaction (ORR) as well as high surface and bulk ionic conductivities [1, 2]. Ionic conductivity of LSCF is one of the highest among perovskites [3, 4]. However according to Tai et al. [5] LSCF shows relatively high thermal expansion coefficient (TEC) in the temperature range 100-600°C (15.3×10^{-6} K^{-1}) which is higher than TEC of zirconia based electrolytes (about 10.0×10^{-6} K^{-1}) and close to TEC of ceria based electrolytes (about 12.5×10^{-6} K^{-1}). Ceria based electrolytes show better ionic conductivity in the intermediate temperature range (500-700°C) than yttria-stabilized zirconia, most frequently used solid electrolyte. In the IT range Ce$_{0.8}$Sm$_{0.2}$O$_{1.9}$ (samaria doped ceria – SDC), Ce$_{0.8}$Gd$_{0.2}$O$_{1.9}$ (gadolinia doped ceria – GDC) and ceria doped by two cations are the most frequently used electrolyte materials [6-8]. Zirconia electrolytes react with cathode materials containing cobalt which results in the appearance of insulating phase. No such reactions were observed in the case of ceria electrolytes.

Electrochemical impedance spectroscopy (EIS) is a powerful method allowing the evaluation of the performance of prepared cathodes. Both charge transfer resistances and the diffusional impedance may be measured by EIS. EIS is also used in the study of the mechanism of oxygen reduction reaction (ORR) although well practice is to confirm the conclusion drawn from EIS using another electrochemical method. Adler et al. [2] proposed mathematical description of the ORR mechanism on porous cathodes. The model (Adler Lane Steel model) they described predicted the Gerisher impedance shape of the electrode impedance spectra and confirm it in the case of the LSCF cathode at 700°C. The other description of ORR on LSCF cathode was presented by Wang et al. [9]. They divided the whole ORR reaction into 6 consecutive steps and deduced the dependency of resistances on the oxygen partial pressure for each step. They presented the EIS spectra containing more futures than Adler et al. [2]. Properties of LSCF cathodes depend not only on strontium or cobalt contents but also on the grain sizes, porosity, oxygen vacancy concentration and on the sintering time and temperature. The last two parameters

*   JERZY HABER INSTITUTE OF CATALYSIS AND SURFACE CHEMISTRY PAS, 30–239 CRACOW, POLAND

** AGH – UNIVERSITY OF SCIENCE AND TECHNOLOGY, FACULTY OF FUELS AND ENERGY, AL. A. MICKIEWICZA 30, 30-059 KRAKÓW, POLAND

can change area specific resistance by up to two orders of magnitude [4]. LSCF cathode material can be improved by addition of some electrolyte material or noble metals: GDC [10], GDC and palladium [10, 11], GDC and silver [12, 13], SDC and silver [14], Ag, Cu, Pt [15] and silver [12, 15-19].

In our previous paper [20] describing preliminary results we found that application of simple impregnation method allowed us to prepare the composite cathode Ag-LSCF with improved performance compared to LSCF monophasic material. The comparative tests performed at 700°C with solid oxide fuel cells Ag-LSCF|SDC|Ni–GDC and LSCF|SDC|Ni-SDC showed the increase of current and power density about by 33% for the cell containing silver as compared to cell involving monophasic cathode material.

The present work describes in more detailed manner the composite Ag-LSCF obtained by impregnation method as well as preparation and characterization of sandwich type composite cathode composed of LSCF layer and silver interlayer placed between LSCF cathode and the electrolyte. The characteristics of the composite Ag-LSCF material as components of solid oxide fuel cell operating in lower temperature range is presented and discussed.

2. Experimental

2.1. Materials preparation

LSCF was prepared from nitrate solution by Pechinni method. The starting materials were: La_2O_3 (99.9%, ACROS), $Sr(NO_3)_2$, $Fe(NO_3)_3 9H_2O$ (99%, POCH), $Co(NO_3)_2 6H_2O$ (99%, POCH), citric acid (99.5%, POCH) and ethylene glycol (99.9%, POCH). Lanthanum nitrate was prepared by dissolving lanthanum oxide in nitrate acid (65%, POCH). The reagents were mixed in distilled water at the proportions enabling preparation of solid solution with the formula $La_{0.6}Sr_{0.4}Co_{0.8}Fe_{0.2}O_{3-\delta}$. Citric acid and ethylene glycol were added to the respective nitrate solutions. Water from the solutions was then evaporated at 180°C for 12 h, then at 200°C for next 12 h and lastly at 220°C for 12 h to remove gaseous reactants. Obtained material was then calcined at 1100°C for 3 h and then rotary-vibratory milled with a zirconia grinding media in dry ethanol.

The electrode was made from LSCF powder by screen printing method for testing the performance of obtained electrode material. Electrodes were prepared on the SDC electrolyte using ethylocelulose (ethoxyl content 49%, 100 cps, Sigma-Aldrich) as pore former and terpineol (Sigma-Aldrich) then calcined at 1100°C for 3 hours. Two different procedures were used to prepare composite materials LSCF-Ag. In the first one silver was introduced into porous structure of LSCF in the form of the solution containing silver nitrate (99.9%, POCH), citric acid and ethylene glycol then the electrode material was dried and calcined at 800°C. The procedure was similar to described in [20]. In the second procedure firstly the silver interlayer was put on the surface of SDC electrolyte and on the top of silver the LSCF cathode was deposited.

2.2. Solid oxide fuel cell preparation

The SDC sintered samples were tested as oxide membranes in a two-chamber solid oxide fuel cell. An anode (50 wt%. NiO-GDC) powder (supplied by Fuel Cell Materials, USA) was mixed with terpineol and ethyl cellulose to form a slurry, subsequently screen-printed on the SDC electrolyte as an anode, then heated at 1200°C for 1 h. The LSCF powder was ground in a rotary-vibratory mill in dry ethylene alcohol using zirconia-grinding media. The ground LSCF powder was mixed with terpineol and ethyl cellulose to form an ink. The ink was screen-printed through a 100-mesh silk screen onto the SDC surface and heated at 400°C for 2 h to remove organic binders then heated at 950°C for 12 h with a heating and cooling rate of 2°/min. For the modification of the LSCF cathode with silver, a method of the nitrate decomposition was applied. 0.05 mol dm^{-3} $AgNO_3$ solution was dropped using a suction pipette with an accuracy of 0.01 ml and poured into the porous LSCF cathode layer placed on the heated hotplate to evaporate water, following by firing at 800°C for 6 h. In the second procedure the Ag thin layer from commercial paste (Electroscience, UK) was deposited on the surface of SDC electrolyte. Then, after drying Ag paste, the LSCF paste was pasted on the top of the metallic layer. The layered composite cathode materials were fired at 900°C for 1 h.

To prepare the Ag modified LSCF cathode, the firing temperature was limited by the melting temperature of Ag (961°C) to prevent agglomeration of the Ag species, which can block the transport path for gaseous oxygen. Thus, the temperature was lower than commonly used sintering temperatures of screen-printed LSCF cathodes, typically between 1000 and 1200°C. The cathode layer adhered well to the electrolyte layer. The low temperature melting of Ag improves the adhesion of the LSCF cathode, and the ceramic impeded grain growth of Ag to some extent.

2.3. Methods

The phase composition of all powders and sintered samples was identified by X-ray diffraction (XRD) analysis basing on the ICDD data base. XRD measurements were performed using the Panalytical X'Pert Pro system with monochromatic Cu K_a radiation. The microstructure observations were carried out using scanning electron microscope (SEM) using the apparatus JEOL JSM-7500F with INCA PentaFetx3 EDS system.

2.4. Electrochemical Impedance Spectroscopy (EIS) measurements

The three electrode setup was used. The silver wire of the diameter 1 mm of the shape of a flat spiral was used as a counter electrode. Platinum foils contacted electrodes were used as current collectors. All three electrodes were joined together by pressing with an alumina rod pressed in turns by a spring located in the cold space. The alumina test fixture was described in our previous work [21]. The EIS measurements were performed using Gamry 300 series potentiostat/galvanostat/ZRA (Gamry Instruments, USA), in oxygen and oxygen-argon atmospheres at the oxygen partial pressure from 0.001 to 1 atm. and temperature 600 and 550°C. The frequency range used in the EIS measurements was from 0.01

to 300000 Hz. The amplitude of the sinusoidal voltage signal was 5 mV. In the analysis of the impedance data the program Minuit [22] based on a non-linear least-square regression procedure, adjusted to treat impedance data was used to fit the equation describing the assumed equivalent electrical circuit (EEC) to the measured data. The quality of the fit was characterized by the standard deviation s, calculated from the formula:

$$s = \sqrt{\frac{\sum_{1}^{n}\left(\frac{\text{Modulus}(Z_{i,measured} - Z_{i,fitted})}{\text{Modulus}(Z_{i,measured})}\right)^2}{n-1}} \qquad (1)$$

where Z_i means the impedance at the frequency number i and n is the number of frequencies in the impedance spectrum.

2.5. Electrochemical tests of solid oxide fuel cells

The following button type solid oxide fuel cells were tested:

H$_2$|Ni-GDC|SDC|LSCF|O$_2$
H$_2$|Ni-GDC|SDC|LSCF–Ag|O$_2$
H$_2$|Ni-GDC|SDC|Ag|LSCF|O$_2$

The apparatus and procedure of electrochemical tests were described in our previous paper [20]. The current and voltage (I-V), power and current (P-I) characteristics were measured by cyclic voltamtery using electrochemical station Autolab connected with 20A Booster.

3. Results and discussion

3.1. XRD

The XRD analysis showed that application of Pechinni method allowed preparation of a monophasic LSCF cathode material. Only the reflexes that may be ascribed to either Ag or LSCF phases were observed in the diffraction patterns of composite materials which confirms that no foreign phases due to the reaction between the AgNO$_3$ solution and LSCF were formed (Fig. 1).
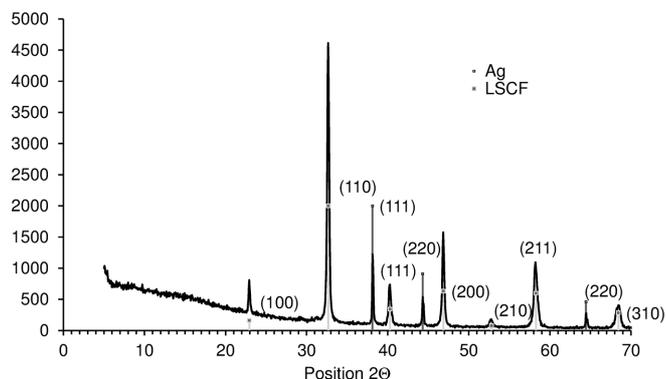

Fig. 1. XRD test of the absence of reaction between LSCF and AgNO$_3$ solution. Grey reflexes originate from LSCF and the dark grey ones from metallic silver

3.2. EIS experiments on LSCF-Ag cathode

The EIS spectra of LSCF-Ag electrodes recorded at 600°C are presented in Fig. 2a. The shape of the spectra reveal three capacitive arcs. The electrolyte arc is not visible due to the frequency limitation and it is represented by resistance R_0 in the electric equivalent circuit (EEC) presented in Fig. 2b. Each visible arc is represented by the pair of resistor and constant phase element (CPE). All three capacitive arcs are oxygen concentration dependent. The diameters of high and middle frequency arcs: represented by (R_1, CPE_1) and (R_2, CPE_2) pairs weakly depend on oxygen concentration whereas the low frequency arc (R_3, CPE_3) invisible in pure oxygen and 50% oxygen grows with the decrease of the oxygen concentration. These diameters of semicircles reflects the resistances R_1, R_2 and R_3. The fitted values of R_1, R_2 and R_3 are proportional to $(P_{O2})^n$ where n are equal –0.0033, –0.0055 and –0.167 respectively. The coefficient n for R_3 is close to –0.125, the value expected by Wang et al. [9] for following reaction:

$$O^- + e^- \rightarrow O^{2-} \qquad (2)$$
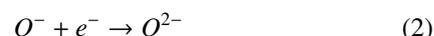
proceeding at the electrode|electrolyte interface as the rate determining step. The middle frequency arc has a shape similar to the Gerisher impedance and can be interpreted by Adler Lane Steel model although we used the pair (R_2, CPE_2) instead of the Gerisher impedance element in EEC and we obtained standard deviations s between 0.18 and 0.72%.
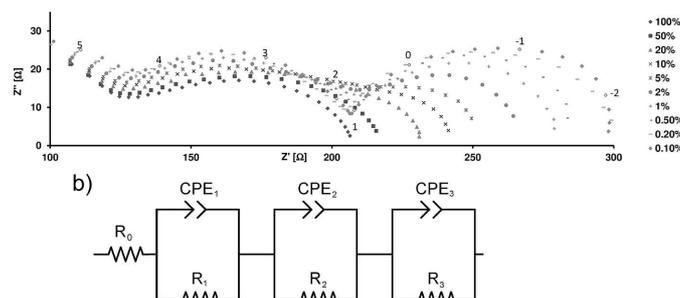

Fig. 2. a) Impedance spectra of the Ag-LSCF electrode on SDC electrolyte at 600°C in oxygen and different oxygen argon atmospheres, the numbers near symbols denote the logarithm of frequency; b) equivalent electrical circuit

3.3. SEM micrographs of composite cathode Ag-LSCF

Fig. 3 presents the SEM microphotographs of the Ag-LSCF composite cathode. Silver crystals of the size up to 5 μm are randomly distributed on the surface of the porous LSCF material. In the larger magnification the small silver particles of the size 10 nm are visible. These particles decorate the whole LSCF matrix.

3.4. Electrochemical tests of solid oxide fuel cells

Figs. 4a-c shows the family of curves (V-I) and (P-I) for cells (1-3) in the temperature range 500-700°C. As can be seen for all investigated cells the open circuit voltage was close to 1 V values calculated from Nernst equation. In all cases the increase of current and power density was observed for solid oxide fuel cell with composite cathode LSCF-Ag in comparison to cathode made from LSCF only. One of the reasons of such behavior may be the improvement of ORR kinetic on the cathodic side.
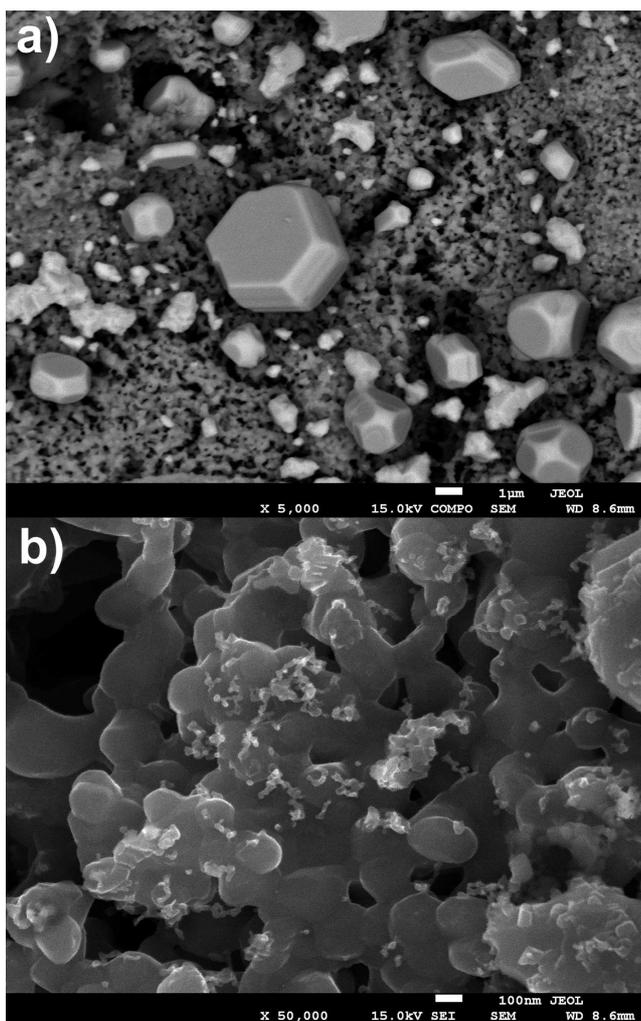
Fig. 3. SEM micrographs of Ag-LSCF composite cathode: a) silver crystals on the surface; b) small silver agglomerates

Direct comparison of performance of both button solid oxide fuel cells involving composite cathode LSCF-Ag with each other showed that the introduction of Ag as interlayer between solid oxide electrolyte SDC and cathode LSCF caused the higher improvement.

4. Conclusions

The shape of the EIS spectra measured on Ag-LSCF electrode indicate that ORR on that electrode may proceeds through at least three slow steps, the low frequency arc can be ascribed to oxidation O^- to O^{2-} ion at the electrode|electrolyte interface. Ag-LSCF|SDC|Ni-GDC and Ni|-GDCSDC|Ag|LSCF reveal greater power output than Ni|SDC|LSCF cell in the 500-750°C temperature range by 14-18% and 18-28% respectively.
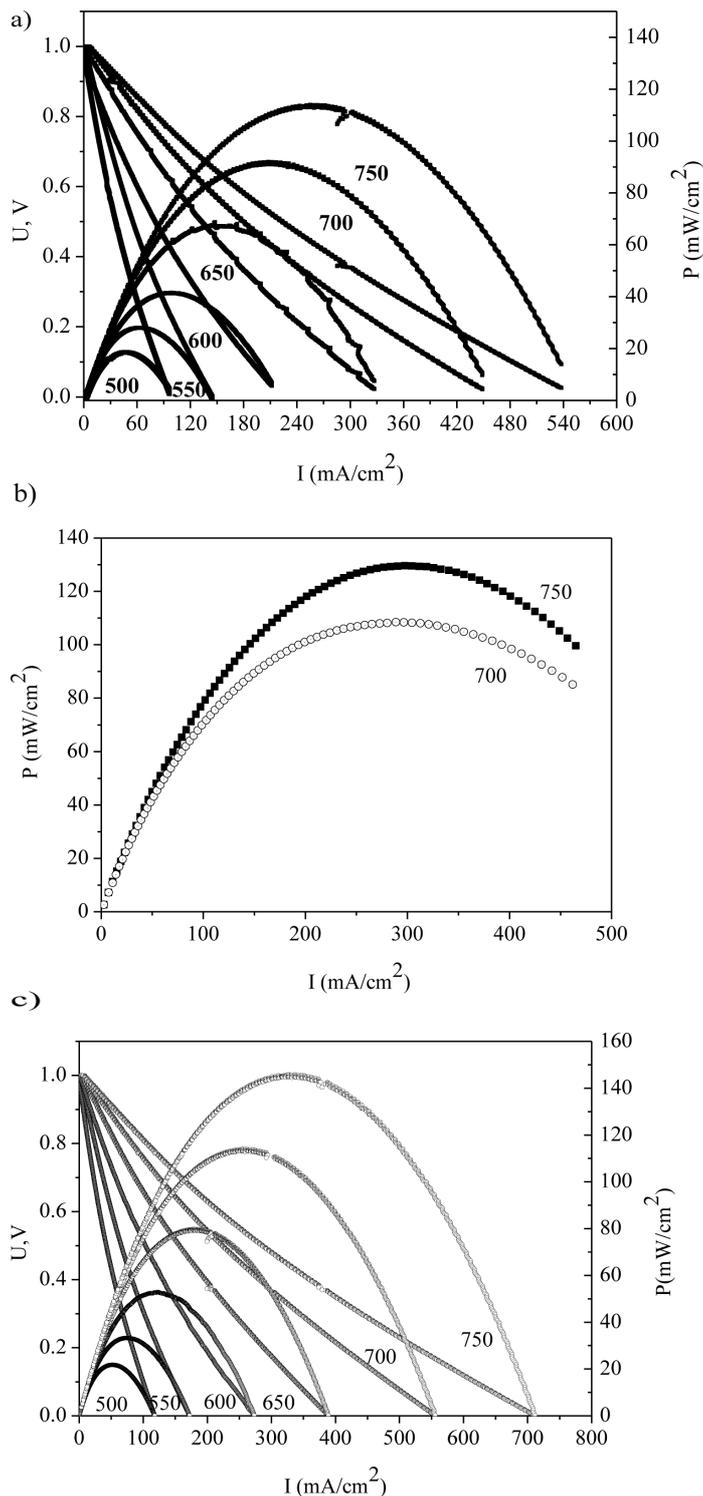
Fig. 4. The family of P-I curves recorded in the temperature range 500-750°C with SDC as a solid electrolyte with: a) monophasic LSCF cathode; b) composite Ag-LSCF cathode c) LSCF cathode with the silver interlayer

REFERENCES

[1] B.C.H. S t e e l e, J.M. B a e, Solid State Ionics **106**, 255 (1997).

[2] S.B. A d l e r, J.A. L a n e, B.C.H. S t e e l e, J. Electrochem. Soc. **143**, 3554 (1996).

[3] V. Dusastre, J.A. Kilner, Solid State Ionics **126**, 163 (1999).

[4] E.V. Tsipis, V.V. Kharton, J. Solid State Electr. **12**, 1367 (2008).

[5] L.W. Tai, M.M. Nasrallah, H.U. Anderson, D.M. Sparlin, S.R. Sehlin, Solid State Ionics **76**, 273 (1995).

[6] J.W. Fergus, J. Power Sources **189**, 30 (2006).

[7] S. Pinol, M. Morale, F. Espirell, J. Power Sources **169**, 2 (2007).

[8] M. Dudek, A. Rapacz-Kmita, M. Mroczkowska, M. Mosiałek, G. Mordarski, Electrochim. Acta **55**, 4387 (2010).

[9] Y. Wang, L. Zhang, F. Chen, C. Xia, J. Hydrogen Energy **37**, 8582 (2012).

[10] S. Wang, T. Kato, S. Nagata, T. Honda, T. Kaneko, N. Iwashita, M. Dokiya, Solid State Ionics **146**, 203 (2002).

[11] S. Wang, T. Kato, S. Nagata, T. Kaneko, N. Iwashita, T. Honda, M. Dokiya, Solid State Ionics **152-153**, 477 (2002).

[12] Y. Sakito, A. Hirano, N. Imanishi, Y. Takeda, O. Yamamoto, Y. Liu, J. Power Sources **182**, 476 (2008).

[13] K. Murata, A. Hirano, N. Imanishi, Y. Takeda, ECS Transactions, **25**, 2413 (2009).

[14] J. Zhang, Y. Ji, H. Gao, T. He, J. Liu, J. Alloy. Compd. **395**, 322 (2005).

[15] J.T. Huang, X.D. Shen, C.L. Chou, J. Power Sources **187**, 348 (2009).

[16] S.P. Simner, M.D. Anderson, J.E. Coleman, J.W. Stevenson, J. Power Sources **161**, 115 (2006).

[17] S.P. Simner, M.D. Anderson, J.W. Templeton, J.W. Stevenson, J. Power Sources **168**, 236 (2007).

[18] Y. Liu, M. Mori, Y. Funahashi, Y. Fujishiro, A. Hirano, Electrochem. Commun. **9**, 1918 (2007).

[19] S.H. Jun, Y.R. Uhm, R.H. Song, C.K. Rhee, Curr. Appl. Phys. **11**, S305 (2011).

[20] M. Mosiałek, M. Dudek, J. Wojewoda-Budka, Arch. Metall. Mater. **58**, 275 (2013).

[21] M. Mosiałek, E. Bielańska, R.P. Socha, M. Dudek, G. Mordarski, P. Nowak, J. Barbasz, A. Rapacz-Kmita, Solid State Ionics **225**, 755 (2012).

[22] F. James, M. Roos, Comput. Phys. Commun. **10**, 343 (1975).